nature geoscience
SUPPLEMENTARY INFORMATION
DOI: 10.1038/NGEO684

Supplementary Information

to: "Deep creep as a cause for the excess seismicity along the San Jacinto Fault" by Shimon Wdowinski

Supplementary figures and a table

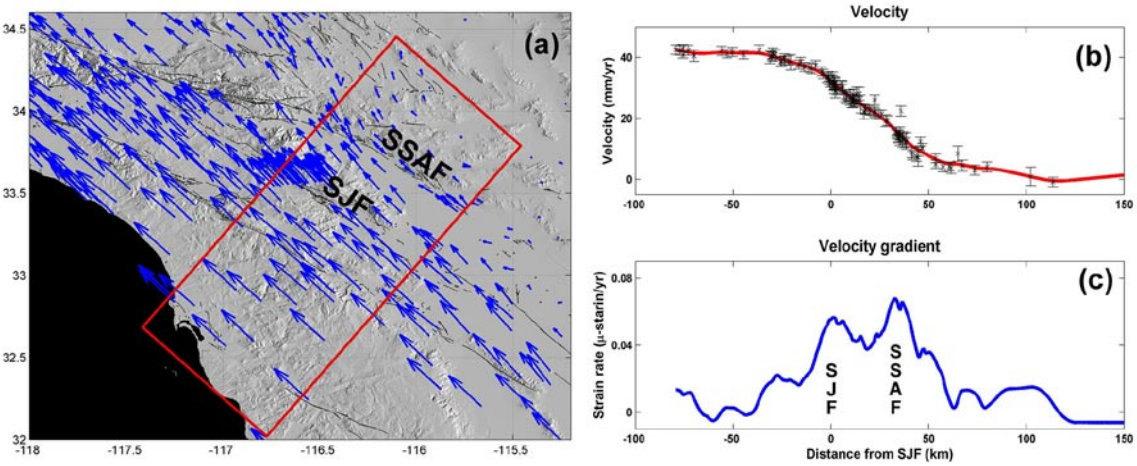

Figure S1: (a) The SCEC crustal motion map, version 3.0[1]. The map shows geodetic determined crustal movements with respect to the stable North America reference frame. The red box marks the location of the velocity vectors used in the velocity profile. (b) A NE-SW transect showing the transition of crustal movements from stable North America to the Pacific plate across the southern San Andreas Fault System (SSAFS). The figure shows the velocity component parallel to the direction of Pacific-North America relative plate motion. The red line marks a best fit curve using a zero offset digital filter. (c) Velocity gradient across the SSAFS showing high strain rates along the San Jacinto Fault (SJF) and Southern San Andreas Fault (SSAF).

DOI: 10.1038/NGEO684

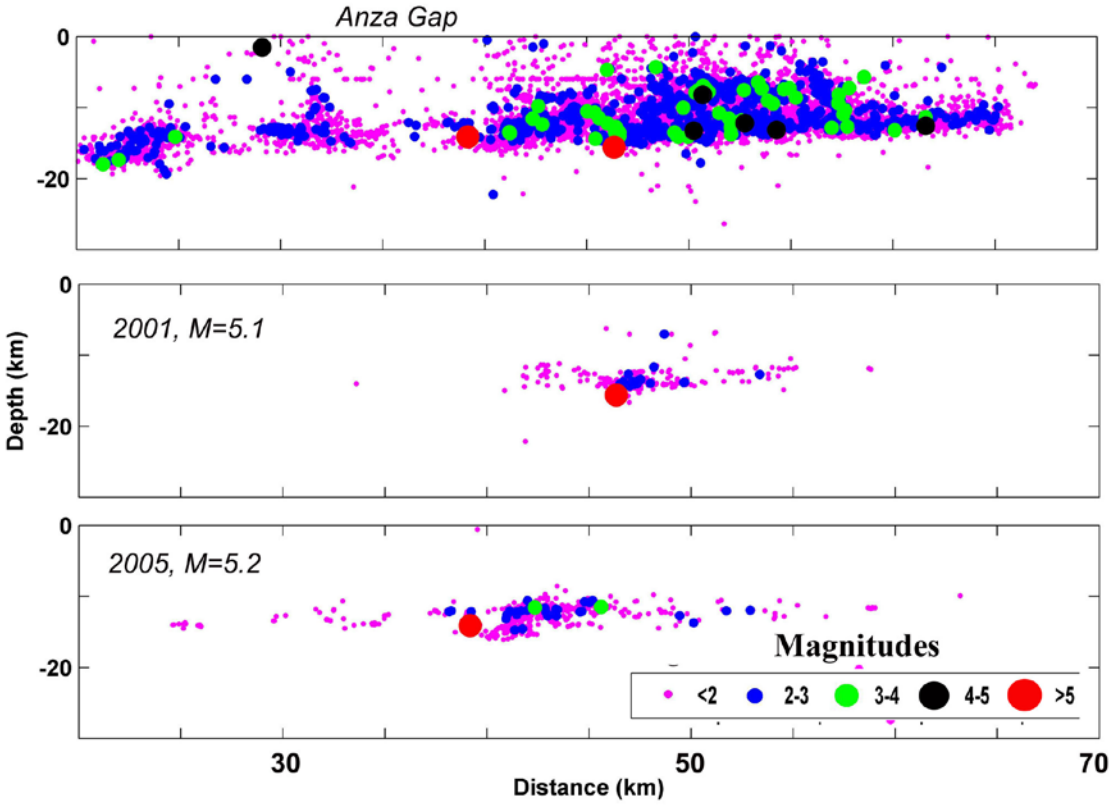

Figure S2: (a) Seismic activity in the north-central part of the central segment, along and south of the Anza Gap, showing excess activity in the 20 km south of the gap at depth of 12-17 km. (b and c) Seven day aftershock activity following the 2001 and 2005 M>5 earthquakes. Each of the two main events occurred at depth of 14-15 km and followed by hundreds of aftershock events, most at depth 12-15 km. The elongated pattern of aftershock activity extending over a 15-20 km long region is atypical for most magnitude 5 earthquakes. It reflects triggered seismic strain release in the deep creep zone.

Table S1: Geodetic determined slip rates and locking depths of the Southern San Andreas and San Jacinto faults

Reference	Southern San Andreas Fault		San Jacinto Fault	
	Slip rate (mm/yr)	Locking depth (km)	Slip rate (mm/yr)	Locking depth (km)
Feigl et al. (1993)[3]	19	15 (assumed)	10	10 (assumed)
Johnson et al. (1994)[4]	25	10	13	5
Bennet et al. (1996)[5]	22 ± 2	12 ± 3	9 ± 2	7.5 ± 1
Smith and Sandwell (2003)[6]	28	22.6 ± 1.7	12	13.1 ± 2.3
Becker et al. (2005)[7]	23.0 ± 8	15 (assumed)	15.3 ± 11	15 (assumed)
Fay and Humphreys (2006)[8]	21.4 ± 0.5	15 (assumed)	15.2 ± 0.9	15 (assumed)
Fialko (2006)[9]	25 ± 2	17 ± 3	21 ± 2	12 ± 3
Smith and Sandwell (2006)[10]	25	23 (assumed)	12	13 (assumed)
Wdowinski et al. (2007)[11]	25	15.8	12-15	9.2
Lundgren et al. (2009)[12]	17 ± 2	15 (assumed)	24 ± 13	15 (assumed)

DOI: 10.1038/NGEO684

Table summary:
Table S1 shows a wide range of slip rate and locking depth estimates for both the SSAF and the SJF. Most studies suggest that the slip rate of the SSAF is higher than that of the SJF. The GPS and other ground based measurement studies show that the slip rate along the SSAF (19-28 mm/yr) is almost double than that of the SJF (10-15 mm/yr). The more recent studies (Fialko, 2006; Lungdern et al., 2009) that use both GPS and InSAR observations suggest that the slip rate along the SJF is similar or even higher than that of the SSAF. Locking depth is often hard to determine and, hence, is assumed by some studies. Most studies that did calculate locking depth indicate that the depth along the SSAF (10-23 km) is 5-6 km deeper than the locking depth of the SJF (5-13 km). Early studies (Johnson et al., 1994; Bennett et al., 1996) are based on limited data and consequently resolve very shallow depths. The two recent studies that determined locking depth along the two faults (Fialko, 2006; Wdowinski et al., 2008) suggest that the locking depth along the SSAF is 16±2 km and along the SJF is 11±2. These two values are used in current study.

References

1. Shen, Z.-K. et al. The SCEC Crustal Motion Map, Version 3.0. (2003).
2. Lin, G. Q., Shearer, P. M. & Hauksson, E. Applying a three-dimensional velocity model, waveform cross correlation, and cluster analysis to locate southern California seismicity from 1981 to 2005. Journal Of Geophysical Research-Solid Earth 112 (2007).
3. Feigl, K. L. et al. Space Geodetic Measurement Of Crustal Deformation In Central And Southern California, 1984-1992. Journal Of Geophysical Research-Solid Earth 98, 21677-21712 (1993).
4. Johnson, H. O., Agnew, D. C. & Wyatt, F. K. Present-Day Crustal Deformation In Southern California. Journal Of Geophysical Research-Solid Earth 99, 23951-23974 (1994).
5. Bennett, R. A., Rodi, W. & Reilinger, R. E. Global positioning system constraints on fault slip rates in southern California and northern Baja, Mexico. Journal Of Geophysical Research-Solid Earth 101, 21943-21960 (1996).
6. Smith, B. & Sandwell, D. Coulomb stress accumulation along the San Andreas Fault system. Journal Of Geophysical Research-Solid Earth 108 (2003).
7. Becker, T. W., Hardebeck, J. L. & Anderson, G. Constraints on fault slip rates of the southern California plate boundary from GPS velocity and stress inversions. Geophysical Journal International 160, 634-650 (2005).
8. Fay, N. & Humphreys, E. D. Fault slip rates, effects of elastic heterogeneity on geodetic data, and the strength of the lower crust in the Salton Trough region, southern California. Journal of Geophysical Research 110, doi:10.1029/2004JB003548 (2005).

9. Fialko, Y. Interseismic strain accumulation and the earthquake potential on the southern San Andreas fault system. Nature 441, 968-971 (2006).
10. Smith, B. R. & Sandwell, D. T. A model of the earthquake cycle along the San Andreas Fault System for the past 1000 years. J. Geophys. Res. 111 (2006).
11. Wdowinski, S., Smith-Konter, B., Bock, Y. & Sandwell, D. Diffuse interseismic deformation across the Pacific-North America plate boundary. Geology 35, 311-314 (2007).
12. Lundgren, P., Hetland, E. A., Liu, Z. & Fielding, E. J. Southern San Andreas-San Jacinto fault system slip rates estimated from earthquake cycle models constrained by GPS and interferometric synthetic aperture radar observations. Journal Of Geophysical Research-Solid Earth 114 (2009).